

Supplemental Material

Methods

Laboratory Analyses

We measured levels of serum and urine electrolytes and creatinine in samples obtained from all patients using routine methods. Intact parathyroid hormone (iPTH) levels were measured by chemiluminescent immunoassay (CLIA Immulite 2000XP, Siemens, Germany), FGF-23 plasma concentrations were determined by ELISA (Human FGF23 C-terminal Elisa kit, Immotopics International, San Clemente, CA, USA) (reference range 26-110 kRU/mL)(for details see below), 25-OH-D₃ was measured by a direct competitive chemiluminescent immunoassay (CLIA, Liaison Analyzer, Diasorin S.p.A.), and 1,25-(OH)₂D₃ was measured after purification by radioimmunoassay (IDS kit, Immunodiagnostic Systems, Germany).

Tubular phosphate reabsorption

Renal phosphate handling was assessed according to Stark et al. as $TmP/GFR = S_{PO4} - (U_{PO4} \times S_{Cr} / U_{Cr})^1$. For S_{PO4} and TmP/GFR , age dependent reference values were used^{1,2}. Mean and SD for TmP/GFR were converted to mmol/L GFR resulting in the following reference ranges (mean \pm 2SD): Newborn=1.4-3.0mmol/l; 1month to 2years = 0.9-2.1mmol/l, 2-12years = 1.0-1.8mmol/l, 12-16years = 0.9-1.7mmol/l, >16years = 0.8-1.2mmol/l.

Genome wide linkage / LOD score calculation

DNA of four affected individuals shown in the pedigrees F1, F2, F3 (Figure S1) was used to map the disease locus. Individuals F1.1, F1.2 and F2.1 were analyzed using Illumina Human660W-Quad BeadChips, individual F3.1 was run on a Human OmniExpress BeadChip. For combined analysis only those SNPs present on both chip types were used where a genotype was obtained for all four individuals (about 239.000 SNPs). Due to the very dense SNP map, some series of SNPs may create a small homozygous region just by chance or since they represent a major haplotype in the population. Those sites will show high LOD score spikes, despite not representing true candidate regions. This phenomenon occurs since the

multipoint calculation by the software has an effect like creating a very low haplotype frequency within that homozygous SNP series by multiplication of the individual allele frequencies. To avoid resulting inflationally high LOD scores in small series of homozygous SNPs, the number of SNPs used for calculating LOD scores was reduced. To this end, first only those SNPs were included where the minor allele was present in at least one individual (181,351 SNPs). The genome was divided into 1/3 cM (centi-Morgan) slices and from the SNPs within each slice, that one SNP was selected to represent that slice that showed the lowest minor allele frequency of all the SNPs within the slice. Thus, the final set of SNPs consisted of 10299 SNPs. Multipoint LOD scores were obtained using Merlin 1.1.2 and the heterogeneity LOD score (HLOD) was calculated and plotted for all autosomes³.

Preparation of Plasmid Constructs/Mutagenesis

Full-length hSLC34A1 was subcloned into a KSM oocyte expression vector. The G153A, G153V, L155P, C336G, V408E, L475fs, and W488R mutations were then introduced by site-directed mutagenesis using the Quick-Change kit (Stratagene). Mutagenic primers were designed using the Stratagene web based QuickChange® Primer Design software Program. The 91del7 variant was generated in two steps. First, the in-frame 21bp deletion was generated by PCR amplification of the two NaPi-IIa fragments excluding the deletion region. PCR primers contained Xho I/Pvu II (N-terminal fragment) and Nae I/Hind III (C-terminal fragment) respectively. Pvu II and Nae I were introduced at the deletion site. Following amplification, the two NaPi IIa PCR fragments were double digested with Xho I/Pvu II and Nae I/Hind III, respectively. After purification, all fragments were ligated and the resulting construct was amplified. This step generated a t>a point mutation at position 269 of NaPi-IIa, which was then re-converted to the original sequence by a new round of Site-Directed Mutagenesis. XL1-Blue ultracompetent cells were transformed with either the PCR products from the Site-Directed Mutagenesis (point mutations) or the ligation product from the first step of the 91del7 generation. The plasmids containing the generated mutations were isolated using QIAprep Spin Miniprep (Qiagen, 27106) and all mutations were confirmed by sequencing (Microsynth). One clone from each construct was used for the experiments.

For oocyte expression, capped cRNA was synthesized in vitro using Megascript T3 kit (Ambion) in the presence of cap analog (New England Biolabs). To study the expression of

wildtype and mutant NaPi-IIa transporter (SLC34A1) in mammalian cells, both wildtype and mutant NaPi-IIa were fused C-terminally to GFP by subcloning the cDNAs into the pEGFP-C1 vector (Clontech).

Cell culture and transient transfections

Opossum kidney cells (clone 3B/2) were cultured in DMEM / Ham's F-12 medium (1:1) supplemented with 10 % fetal calf serum, 2 mM glutamine, 20 mM HEPES and 50 IU/ml penicillin/streptomycin as previously reported ⁴. Cells were plated on coverslips in 12 multiwell plates (TPP), and cultures were transfected with either wild-type hNaPi-IIa fused to pEGFP-C1 vector or with the mutants described above. Cultures were transfected at about 70 % confluency by an overnight incubation in 500 µl OPTIMEM (GIBCO, 31985-047) containing 1 µg of DNA and 3 µl of Lipofectamine™ 2000 Reagent (Invitrogen, 11668-019). We performed two independent experiments, each in duplicates or triplicates.

Actin staining and confocal microscopy

Upon expression of clear patches of wt NaPi-IIa signal (two to three days after transfection), cells were fixed and permeabilised with saponin as described previously ⁵. Thereafter, actin was stained by incubation with Texas Red®-X phalloidin (Invitrogen) diluted 1:500. After incubation for 30 min in the dark, cells were washed three times with PBS/saponin and once with PBS. The coverslips were then mounted on microscope slides using Dako Glycergel® Mounting Medium. The subcellular final locations of the transfected cotransporters were analysed by Confocal Laser Scanning Microscopy (Leica SP2) using a 63x oil immersion objective at the Center for Microscopy and Image Analysis at the University of Zurich.

Expression of hNaPi-IIa and mutants in *Xenopus laevis* oocytes

Female *X. laevis* frogs were purchased from Xenopus Express (France) or African Xenopus Facility (R. South Africa). Portions of ovaries were surgically removed from frogs anesthetized in MS222 (tricaine methansulphonate) and cut in small pieces. Oocytes were

treated for 45 min with collagenase (crude type 1A) 1 mg/mL in 100Na solution (without Ca²⁺) in presence of 0.1 mg/mL trypsin inhibitor type III-O. Healthy stage V-VI oocytes were selected, maintained in modified Barth's solution at 16°C. All animal procedures were conducted in accordance with the Swiss Cantonal and Federal legislation relating to animal experimentation.

Solutions and reagents

The standard extracellular solution for oocyte experiments (100 Na) contained (in mM): 100 NaCl, 2 KCl, 1.8 CaCl₂, 10 HEPES, pH 7.4 adjusted with Tris. P_i was added from a 1M K₂HPO₄/KH₂PO₄ stock premixed to give pH 7.4. Modified Barth's solution for storing oocytes contained (in mM): 88 NaCl, 1 KCl, 0.41 CaCl₂, 0.82 MgSO₄, 2.5 NaHCO₃, 2 Ca(NO₃)₂, 7.5 HEPES, pH 7.5 adjusted with Tris and supplemented with 5 mg/L doxycyclin and 5 mg/L gentamicin. All standard reagents were obtained from either Sigma-Aldrich or Fluka (Buchs, Switzerland).

³²P_i uptake

Oocytes were injected with 50 nl of cRNA (200 ng/μL) for wild-type (wt) or mutant hNaPi-IIa constructs. Experiments were performed 3 days after injection. Non-injected control oocytes (NI), oocytes expressing hNaPi-IIa wt and mutants (6-10 oocytes/group) were first allowed to equilibrate in 100 Na solution without tracer. After aspiration of this solution, oocytes were incubated in 100 Na solution containing 1 mM cold P_i and ³²P_i (specific activity 10 mCi/mmol P_i, Perkin Elmer). Uptake proceeded for 10 min, then oocytes were washed 4 times with ice-cold 0 Na solution containing 2 mM P_i and lysed individually in 2% SDS for 10 min before addition of the scintillation cocktail. The amount of radioactivity in each oocyte was measured by scintillation counting (Tri-Carb 29000TR, Packard).

Two-electrode voltage clamp experiments

All voltage clamp experiments were performed using a two-electrode voltage clamp (TEC-10CX, NPI, Tamm, Germany). Oocytes were impaled with microelectrodes filled with 3 M KCl, with a typical resistance of <1 MΩ. The temperature of the recording chamber was

monitored using a thermistor probe (TS-2, NPI, Tamm, Germany) placed close to the oocyte. The temperature of the recording chamber and incoming superfusate were regulated using Peltier cooling elements driven by a continuous feedback controller (TC-10, NPI Tamm, Germany). Data acquisition was performed using a 1440 Digidata (Molecular Devices Corp, USA). For recordings at constant holding potential, currents were acquired at >20 samples/s and filtered at 10 Hz. Faster sampling rates (up to 20 k samples/s) were used for voltage step recordings with filtering (digital and analog) adjusted accordingly.

Steady-state currents were obtained using a protocol in which membrane voltage steps were made from the holding potential (V_h) = -60 mV, to test voltages in the range -180 to +80 mV in 20 mV increments. The steady-state P_i -dependent current (I_{P_i}) was obtained by subtracting control traces (in 100 Na solution) from the corresponding traces in the presence of P_i . The current was measured in a region where all presteady-state relaxations were completed. Data was rejected if contaminated by endogenous Cl-currents. Steady state P_i activation was determined by varying the P_i concentration in presence of 100 Na and subtracting the respective currents in 100 Na from those in 100 Na + P_i .

Animal studies

Plasma concentrations of intact parathyroid hormone (iPTH) and intact FGF-23 were determined by ELISA (Immutopics, San Clemente, CA, USA and Kainos, Tokyo, Japan, respectively). The kit to measure PTH contains streptavidin-coated wells together with biotinylated and horseradish peroxidase (HRP)-conjugated antibodies against PTH. For details concerning FGF-23 determination please see below. Renal mRNAs of *Cyp27b1* and *Cyp24a1* were quantified by real time PCR. For that, total RNA purified from kidneys (RNeasy Mini Kit, Qiagen) was incubated with reverse transcriptase (TaqMan Reverse Transcription Kit, Applied Biosystems) to produce cDNA that was then used as template for real time PCR. The expression of both hydroxylases was normalized to the expression of hypoxanthine guanine phosphoribosyl transferase (HPRT) according to the formula $R = 2^{[Ct(HPRT) - Ct(test\ gene)]}$, where R is the relative ratio and Ct indicates the cycle number at the threshold of 0.2. All primers and probes were obtained from Taqman Gene Expression Assays.

Determination of human and mouse FGF-23

For the determination of FGF-23 in patients the Immutopics Human FGF-23 (C-terminal) ELISA kit was used (Immutopics International, San Clemente, CA, USA). FGF-23 in mice was measured using the Kainos intact FGF-23 ELISA kit (TECOmedical AG, Sissach, Switzerland). Both assays are two-step enzyme-linked immunosorbent assays. The Kainos assay only detects full-length or intact FGF-23 (iFGF-23) by using antibodies directed against C- and N-terminal regions of FGF-23. In contrast, the C-terminal antibody used in the Immutopics assay detects both intact FGF-23 as well as processed C-terminal fragments of FGF-23 (cFGF-23) ⁶. Whereas Immutopics recommends to measure cFGF-23 in EDTA plasma, the Kainos iFGF-23 kit can be used with either serum or plasma. However, using serum for measurement of intact FGF-23 potentially yields falsely low concentrations caused by preanalytical instability ⁷.

In general, obtaining reliable FGF-23 values is challenging due to the instability of the FGF-23 hormone. Within hours after blood-taking, levels of intact FGF-23 decrease as a result of protease cleavage, whereas FGF-23 levels measured by C-terminal assay which also detects inactive fragments remains relatively stable over time ⁸. Therefore, immediate separation of plasma or serum and subsequent testing is recommended especially for the determination of iFGF-23. Alternatively, samples may be frozen at -20 °C. As the C-terminal assay detects both iFGF-23 as well as processed C-terminal fragments (cFGF-23), it might be considered less susceptible to suboptimal probe processing (see above). Obtaining falsely lower measured values for FGF-23 would be particularly problematic in patients with a suspected suppression of FGF-23 including patients with NaPi-IIa (*SLC34A1*) or NaPi-IIc (*SLC34A3*) defects. For this reason, the cFGF-23, the parameter considered more stable, was measured in human patients, whereas iFGF-23 was determined in mice where experimental conditions allow for a uniform and rapid sample processing. Previously, FGF-23 levels have been reported in a single family with *SLC34A1* mutations by Magen and colleagues ⁹. They measured iFGF-23 as well as cFGF-23 in their two patients with a homozygous *SLC34A1* mutation and report values at the lower end of the reference ranges for both assays.

Intra- and inter-assay variances for the **Immutopics Human FGF-23 (C-terminal) ELISA kit** (provided in the assay`s manual, copyright Immutopics, Inc., San Clemente, CA, USA):

To assess intra-assay precision the mean and coefficient of variation were calculated from 20 duplicate determinations of two samples each performed in a single assay.

Mean Value (RU/mL)	Coefficient of Variation
33.7	2.4%
302	1.4%

To assess inter-assay precision the mean and coefficient of variation were calculated from duplicate determinations of two samples performed in 10 assays.

Mean Value (RU/mL)	Coefficient of Variation
33.6	4.7%
293	2.4%

Intra- and inter-assay variances for the **Kainos intact FGF-23 (C-terminal) ELISA kit** are provided on the manufacturer`s homepage (www.kainos.co.jp)

(http://www.kainos.co.jp/eng/products/fgf23_e/fgf23_e_4.html)

Intra-assay precision:

Mean Value (pg/mL)	Coefficient of Variation
14.2	3.0%
28.7	2.8%
33.6	2.0%

Inter-assay precision:

Mean Value (pg/mL)	Coefficient of Variation
19.5	3.8%
42.4	2.1%
119	2.4%

Results

Patients

Figure S2:

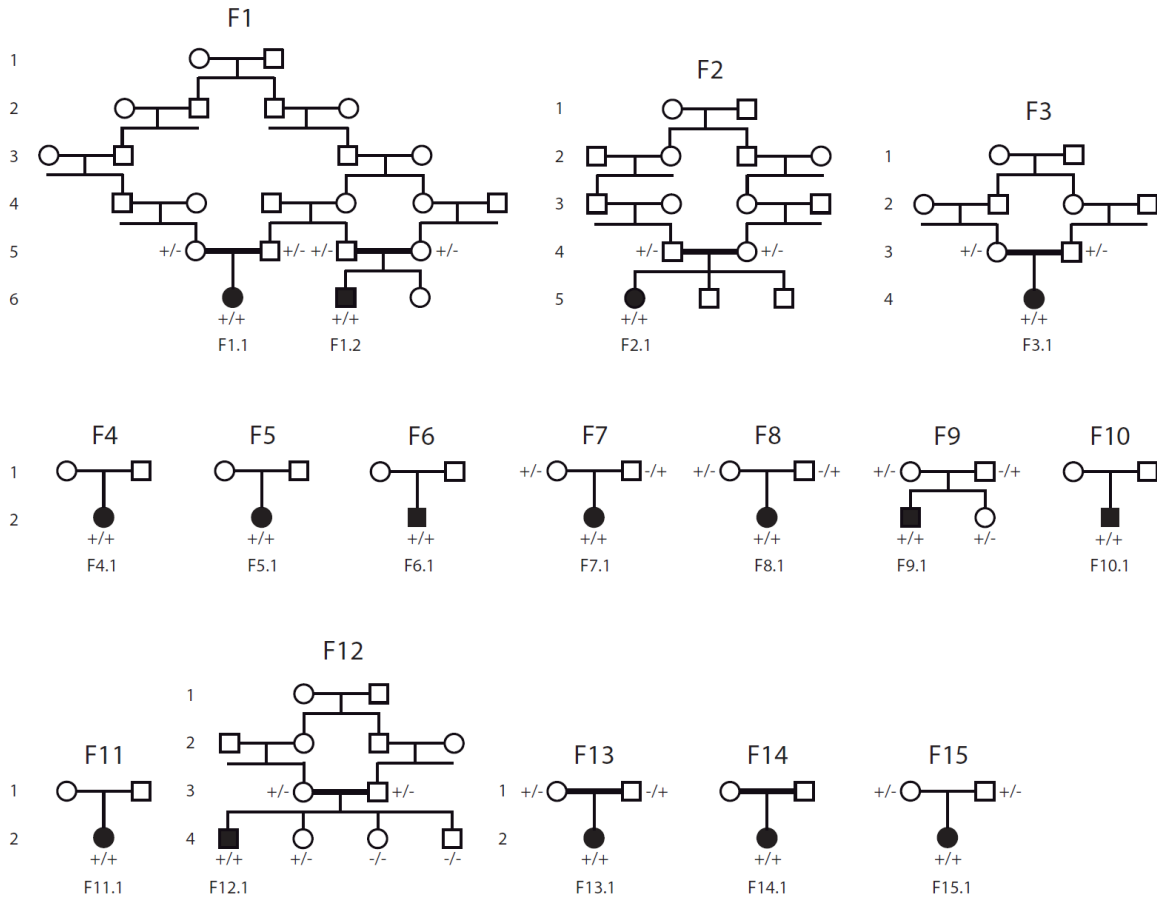


Figure S2: **Pedigrees of IIH families F1 – F15.** Families F1 to F3 with parental consanguinity were used for homozygosity mapping. F4 to F14 represent families with sporadic cases. The patient from family F15 did not present clinically with IIH, but exhibited nephrocalcinosis as an incidental finding. Affected family members are indicated with solid circles (girls) and squares (boys), double horizontal lines indicate parental consanguinity. Mutated alleles are denoted by (+), wild-type alleles by (-).

Genome wide linkage / LOD score calculation

Figure S1:

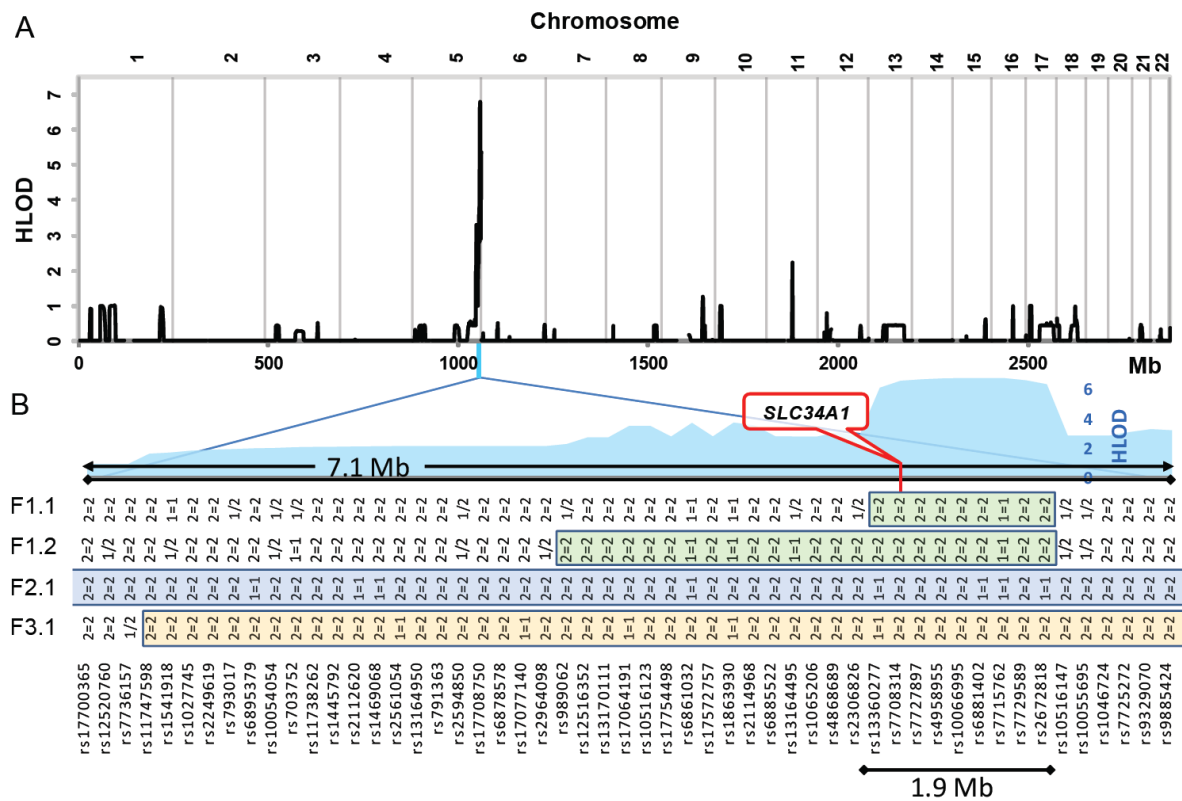


Figure S1. **Linkage analysis.** (A) Multipoint LOD scores were obtained using Merlin 1.1.2 and the heterogeneity LOD score (HLOD) was plotted for all autosomes. The maximum HLOD was 6,791 in a homozygosity region of about 2 Mb close to chromosome 5-qter. (B) The candidate region of panel A zoomed in. At top the HLOD is shown as a blue background area. The GenBank accession numbers of SNPs are given in the bottom line. The genotypes are denoted as "1=1" for homozygous major allele, "2=2" for homozygous minor allele and "1/2" for heterozygous state. The position of the candidate gene *SLC34A1* is indicated. The SNP rs7708314 (C/T, base position 176.809.618 on chromosome 5 [GRCh37], minor allele frequency 0,11) is located close to the *SLC34A1* gene (NM_003052.4: c.-1918C>T). The length of the homozygosity region between the next heterozygous markers used for LOD score calculations is 1,9 Mb. Detailed review including also the markers that were not used for the Merlin-calculations demonstrated that the true homozygosity region is 1,66 Mb (between heterozygous markers rs3762974 and rs185493, not shown).

Table S1. List of candidate gene within the critical interval

SNP rs3762974; Chr5, 176.901.335bp (GRCh38)		
RefSeq genes	Description	RefSeq Acc-No
UIMC1	ubiquitin interaction motif containing 1	NM_016290
ZNF346	zinc finger protein 346	NM_012279
FGFR4	fibroblast growth factor receptor 4	NM_002011
NSD1	nuclear receptor binding SET domain protein 1	NM_022455
RAB24	RAB24, member RAS oncogene family	NM_130781
PRELID1	PRELI domain containing 1	NM_013237
MXD3	MAX dimerization protein 3	NM_031300
LMAN2	lectin, mannose-binding 2	NM_006816
RGS14	regulator of G-protein signaling 14	NM_006480
SLC34A1	solute carrier family 34 (NaPi), member 1	NM_003052
PFN3	profilin 3	NM_001029886
F12	coagulation factor XII (Hageman factor)	NM_000505
GRK6	G protein-coupled receptor kinase 6	NM_002082
PRR7	proline rich 7 (synaptic)	NM_030567
DBN1	drebrin 1	NM_080881
PDLIM7	PDZ and LIM domain 7 (enigma)	NM_005451
DOK3	docking protein 3	NM_024872
DDX41	DEAD (Asp-Glu-Ala-Asp) box polypeptide 41	NM_016222
FAM193B	family with sequence similarity 193, member B	NM_001190946
TMED9	transmembrane emp24 protein transport domain containing 9	NM_017510
B4GALT7	xylosylprotein beta 1,4-galactosyltransferase, polypeptide 7	NM_007255
FAM153A	family with sequence similarity 153, member A	NM_173663
PROP1	PROP paired-like homeobox 1	NM_006261
FAM153C	family with sequence similarity 153, member C	NM_001079527
N4BP3	NEDD4 binding protein 3	NM_015111
RMND5B	required for meiotic nuclear division 5 homolog B	NM_022762
NHP2	NHP2 ribonucleoprotein	NM_017838
HNRNPAB	heterogeneous nuclear ribonucleoprotein A/B	NM_031266
PHYKPL	5-phosphohydroxy-L-lysine phospho-lyase	NM_153373
COL23A1	collagen, type XXIII, alpha 1	NM_173465
Processed transcripts		
ZNF346-IT1	ZNF346 intronic transcript 1 (non-protein coding)	HGNC:41423
CTD-2301A4.3	ribosomal protein L21 (RPL21) pseudogene	
PRMT1P1	protein arginine methyltransferase 1 pseudogene 1	HGNC:49611
CTD-2301A4.1	ribosomal protein S20 (RPS20) pseudogene	
PRR7-AS1	PRR7 antisense RNA 1	HGNC:27961
RP11-1334A24.5	to be experimentally confirmed	
RP11-1334A24.6	putative novel antisense transcript	
RP11-1277A3.1	novel antisense transcript	
RP11-1101H11.1	putative novel antisense transcript	
RP11-1026M7.2	novel transcript antisense to FAM153A	
RP11-423H2.3	novel transcript, antisense to PROP1	
RP11-423H2.4	to be experimentally confirmed	
RP11-423H2.5	novel antisense transcript	
CTB-26E19.1	novel sense intronic transcript	
RP11-1259L22.1	putative novel antisense transcript	
SNP rs185493; Chr5, 178.564.257bp		

Mutational Analysis

Figure S3:

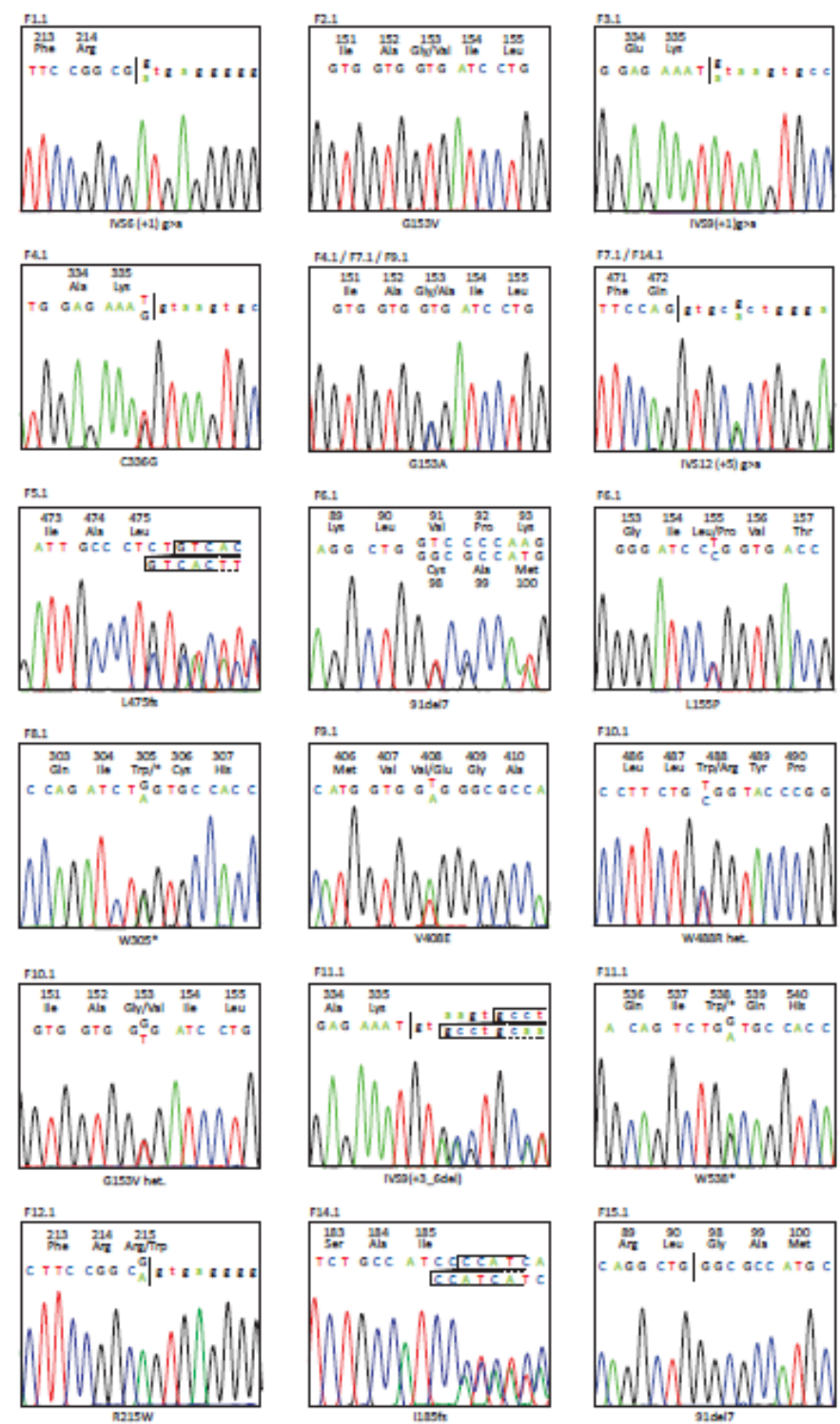


Figure S3. **Electropherograms of identified *SLC34A1* mutations.** Sequencing was performed in affected patients and for cosegregation analysis in available family members. *SLC34A1* mutations appear in homozygous or heterozygous state, respectively. If a mutation was discovered in more than a single patient, a representative electropherogram of one patient is shown. On top, the consequence on protein level is indicated above the corresponding change on nucleotide level.

Clinical data

Table S2

Patient	F1.2	F1.2	F2.1	F3.1	F4.1	F5.1	F6.1	F7.1	F8.1	F9.1	F10.1	F11.1	F12.1	F13.1	F14.1	F15.1
Origin	Turkey	Turkey	Turkey	Turkey	Netherlands	Poland	Poland	Poland	Germany	Germany	Turkey	Bulgaria	Israel	Belgium	Italy	Poland
Age at Presentation	20 days	1 month	2 months	2 months	2 months	4 months	9 months	10 months	1month	3 months	3 months	4 months	7 months	6 months	3 months	18 months
Vitamin D Prophylaxis	400IE	400IE	500IE	400IE	500IU	2000IU	2000IU	400IU	500IU	500IU	200IU	1334IU	200IU	500IU	500IU	800IE
Weight loss/ Failure to thrive	Yes	Yes	No	Yes	Yes	Yes	Yes	Yes	Yes	No	Yes	Yes	No	No	Yes	No
Polyuria/Dehydration	Yes	Yes	No	Yes	No	Yes	Yes	Yes	Yes	No	Yes	Yes	Yes	No	Yes	Yes
Muscular Hypotonia	Yes	No	No	No	No	Yes	Yes	No	No	Yes	No	No	No	No	No	No
Nephrocalcinosis	Yes	Yes	Yes	Yes	Yes	Yes	Yes	Yes	Yes	Yes	Yes	Yes	Yes	Yes	Yes	Yes
Hypercalciuria	Yes	Yes	Yes	Yes	Yes	Yes	Yes	Yes	Yes	No	Yes	No	Yes	No	Yes	No
initial serum calcium (mM)(2.1-2.6)	3.5	2.9	3.1	3.2	3.8	3.1	3.0	3.4	3.4	3.4	2.8	3.6	3.1	2.6	2.8	2.6
initial serum phosphate (mM)	1.0 (-5.8SDS)	0.5 (-8.6SDS)	1.5 (-2.8SDS)	0.7 (-7.2SDS)	1.1 (-5.0SDS)	1.2 (-4.1SDS)	1.3 (-2.8SDS)	1.8 (+0.1SDS)	1.7 (-1.9SDS)	1.0 (-5.4SDS)	0.6 (-7.6SDS)	1.0 (-5.2SDS)	1.0 (-4.7SDS)	1.6 (-1.5SDS)	1.8 (+0.1SDS)	1.7 (+0.4SDS)
TmP/GFR (mmol/L GF)	0.9 (-3.3SDS)	n.d.	1.4 (-0.3SDS)	n.d.	0.9 (-2.0SDS)	1.2 (-1.0SDS)	n.d.	n.d.	1.6 (+0.3SDS)	0.9 (-2.0SDS)	0.5 (-3.3SDS)	n.d.	n.d.	n.d.	n.d.	n.d.
initial PTH (pg/mL) (14-72)	1.0	15	5.5	31	2.8	*	*	<3	4,9	<3	<3	<3	<1	1.9	<3	13
initial 25-OH-D ₃ (ng/mL)(10-65)	28	n.d.	44.6	46.2	20.4	55.7	23.4	33.7	n.d.	56.3	15.9	70	28.1	48.3	n.d.	21
initial 1,25-(OH) ₂ D ₃ (pg/mL)(17-74)	139	n.d.	146.3	25.8	50.8	62.5	82.1	271	n.d.	63.2	n.d.	135	53	131.7	n.d.	32
Therapy (acute phase)	Ketoconazole Phosphate	Rehydration	no	Rehydration Steroids Furosemide	Rehydration	Rehydration Steroids	Rehydration Steroids	Rehydration	Rehydration	Rehydration	Rehydration	Rehydration Steroids Bisphosphonates	Rehydration	Rehydration	Rehydration	no
Therapy (long term)	oral phosphate hydrochlorothiazide	oral phosphate hydrochlorothiazide	no	low calcium diet	no	oral phosphate low calcium diet	oral phosphate low calcium diet	low calcium diet potassium citrate	hydrochlorothiazide	oral phosphate	oral phosphate	no	no	no	potassium citrate	potassium citrate

Follow-up																
Age at last visit	1.5 years	7 years	6 years	1.5 years	14 years	10 years	17 years	3 years	3 years	0.9years	1 year	0.9years	11 years	6 years	1 year	3.5 years
last serum calcium (mM)(2.1-2.6)	2.7	2.5	2.4	2.8	2.7	2.7	2.6	2.6	2.5	2.6	2.6	2.6	2.5	2.5	2.7	2.7
last serum phosphate (mM)	0.9 (-4.1SDS)	1.1 (-1.7SDS)	1.5 (+0.5SDS)	1.8 (+0.9SDS)	1.0 (-2.3SDS)	1.5 (+0.5SDS)	0.9 (-2.8SDS)	1.5 (+0.1SDS)	1.7 (+1.2SDS)	1.5 (-1.6SDS)	1.8 (+0.4SDS)	1.5 (-1.6SDS)	1.2 (-1.2SDS)	1.6 (+1.0SDS)	1.8 (+0.4SDS)	1.7 (+1.3SDS)
TP/GFR (mmol/L GF)	0.8 (-3.0SDS)	1.0 (-2.0SDS)	1.3 (-0.5SDS)	n.d.	0.7 (-3.0SDS)	1.3 (-0.5SDS)	0.7 (-3.0SDS)	1.3 (-0.5SDS)	1.4 (±0.0SDS)	1.4 (-0.5SDS)	1.3 (-1.0SDS)	1.3 (-1.0SDS)	1.1 (-1.5SDS)	n.d.	n.d.	1.6 (+1.0SDS)
last PTH (pg/mL) (14-72)	21	23	20	42	33	21	8.2	6.9	19	12	36	16	7.1	19	10	22
FGF-23 (KRU/L) (26-110)	136	n.d.	n.d.	77	82	29	54	47	114	33	n.d.	n.d.	n.d.	n.d.	n.d.	n.d.
last 25-OH-D ₃ (ng/mL) (10-65)	8	12	26	36	53	22	15	26	16	38	n.d.	63	25	53	n.d.	38
last 1,25-(OH) ₂ D ₃ (pg/mL)(17-74)	57	75	58	n.d.	58	49	53	103	35	59	n.d.	146	n.d.	79	n.d.	54
Mutation <i>SLC34A1</i> (nucleotide level)	c.644(+1) g>a homoz.	c.644(+1) g>a homoz.	C458 G>T homoz.	c.1006(+1) g>a homoz.	c.458 G>C + c.1006 T>G	c.1425_26 del + ?	c.271_91 del + c.464T>C	c.458 G>C + c.1416(+5) g>a	c.271_91 del + c.914 G>A	c.458 G>C + c.1223 T>A	c.458 G>T + c.1462 T>C	c.1006 (+3_6)del + c.1614 G>A	c.644 G>A homoz.	c.271_91 del + c.1223 T>A	c.555_556 del + c.1416(+5) g>a	c.271_91 del homoz.
Mutation NaPi-IIa (protein level)	IVS6(+1)g>a a homoz.	IVS6(+1)g>a a homoz.	p.G153V homoz.	IVS9(+1)g>a homoz.	p.G153A + p.C336G	p.L475fs + ?	p.91del7 + p.L155P	p.G153A + IVS12(+5) g>a	p.91del7 + p.W305*	p.G153A + p.V408E	p.G153V + p.W488R	IVS9(+3_6) del + p.W538*	p.R215W/ (splice site) homoz.	p.91del7 + p.V408E	p.I185fs + IVS12(+5) g>a	p.91del7 homoz.

* = instead of intact PTH, whole PTH was measured and within the lower normal range

Table S2. Full set of clinical, biochemical and genetic data of all 15 patients including sporadic IIH cases. For serum phosphate as well as Tmp/GFR instead of a reference range age-specific SDS are provided according to ¹, for age >16 years adult values were used (= 3.2 (±0.3) identical to the nomogram by Walton/Bijvoet)¹⁰. The c.644G.A mutation in patient F12.1 leads to an exchange of arginine 215 to tryptophane but primarily affects the donor splice site of exon 6.

Table S3. Clinical, biochemical, and genetic data of parents of families F1 and F9.

Family 1	NaPi-IIa mutation	nephrocalcinosis/nephrolithiasis	S-Ca (mmol/L) (2,1-2,6)	S-PO4 (mmol/L) (0,9-1,5)	PTH (pg/mL) (14-72)	25-OH-D ₃ (ng/mL) (10-65)	1,25-OH ₂ -D ₃ (pg/mL) (17-74)	TmP-GFR (mmol/L GF) (0,8-1,4)	Urine Ca/Crea (mg/mg) (<0.25)
father F1.1	IVS6(+1)g>a het.	no	2,5	1,0	42,7	5	56	0,9	0,20
mother F1.1	IVS6(+1)g>a het.	no	2,3	1,0	23,1	11	67	0,8	0,17
father F1.2	IVS6(+1)g>a het.	no	2,4	0,9	23,5	6	54	0,8	0,49
mother F1.2	IVS6(+1)g>a het.	no	2,5	1,1	109	4	60	1,1	0,16
father F9.1	p.G153A het.	no	2,4	0,9	110	34	77	0,8	0,06
mother F9.1	p.V408E het.	no	2,5	0,9	14	20	61	0,8	0,18

Table S4: Available clinical and biochemical data of parents of families F1 to F15.

Obligate Heterozygotes		Genetic Data	Nephrolithiasis	S-Ca (mmol/L)	S-PO4 (mmol/L)	PTH (pg/mL)
F1.3	father F1.1	IVS6(+1)g>a het.	no	2,5	1,0	42,7
F1.4	mother F1.1	IVS6(+1)g>a het.	no	2,3	1,0	23,1
F1.5	father F1.2	IVS6(+1)g>a het.	no	2,4	0,9	23,5
F1.6	mother F1.2	IVS6(+1)g>a het.	no	2,5	1,1	109
F3.2	father	IVS9(+1)g>a het.	no	2,6	1,5	45,5
F3.2	mother	IVS9(+1)g>a het.	no	2,5	1,4	38,6
F4.2	father	-	no	-	-	-
F4.3	mother	-	no	-	-	-
F5.2	father	-	yes	2,3	-	18
F5.3	mother	-	yes	2,4	-	-
F7.2	father	p.G153A het.	no	2,2	0,9	23,4
F7.3	mother	IVS12(+5)g>a het.	no	2,3	1,2	55,1
F8.2	father	p.W305* het.	no	-	-	-
F8.3	mother	p.91del7 het.	no	-	-	-
F9.2	father	p.G153A het.	no	2,4	0,9	110
F9.3	mother	p.V408E het.	yes	2,5	1,0	14
F10.2	father	-	no	-	-	-
F10.3	mother	-	no	-	-	-
F11.2	father	-	no	-	-	-
F11.3	mother	-	no	-	-	-
F13.2	father	-	no	2,2	0,6	3
F13.3	mother	-	no	2,4	1,2	-
F14.2	father	-	no	-	-	-
F14.3	mother	-	no	-	-	-
F15.2	father	p.91del7 het.	no	-	-	-
F15.3	mother	p.91del7 het.	no	-	-	-
			3/26	2.4 (2.2-2.6) (n=14)	1.0 (0.6-1.5) (n=12)	32 (3-110) (n=12)

Animal data

Table S4:

Serum/Plasma and Urine parameters:

	<i>Slc34a1</i> ^{-/-}			<i>Slc34a1</i> ^{+/+}		
	LowP, highD	LowP, lowD	HighP, lowD	LowP, highD	LowP, lowD	HighP, lowD
Serum/Plasma						
Pi (mmol/L)	0.90 ± 0.03**	0.98 ± 0.12 ^{ns}	2.08 ± 0.20 ^{oo}	1.88 ± 0.25	1.64 ± 0.22	2.93 ± 0.30
Ca ²⁺ (mmol/L)	3.23 ± 0.23*	2.97 ± 0.12 ^{ns}	2.05 ± 0.08 ^{ooo}	2.84 ± 0.12	2.97 ± 0.24	1.86 ± 0.25
PTH (pg/ml)	36.9 ± 0.3 ^{ns}	37.6 ± 0.6 ^{ns}	392.1 ± 175.0 ^{ns}	40.3 ± 1.4	48.1 ± 13.1	91.3 ± 15.6
FGF23 (pg/ml)	14.2 ± 1.6*	11.8 ± 1.9 ^{ns}	51.8 ± 13.3 ^o	570.6 ± 222.2	18.8 ± 0.9	108.2 ± 48.1
25-OH- D ₃ (ng/ml)	200.8 ± 24.7 ^{ns}	12.8 ± 0.7 ^{ns}	16.1 ± 1.3 ^{ns}	165.2 ± 14.6	11.5 ± 0.8	16.7 ± 1.4
1,25-(OH) ₂ D ₃ (pg/ml)	16.5 ± 2.5*	64.4 ± 8.4 ^{ns}	30.3 ± 3.6 ^{ns}	7.4 ± 1.0	44.9 ± 6.0	35.2 ± 3.7
<i>Cyp27b1</i> mRNA *	0.110 ± 0.021**	0.411 ± 0.077 ^{oo}	0.040 ± 0.004 ^o	0.005 ± 0.001	0.290 ± 0.024	0.060 ± 0.007
<i>Cyp24a1</i> mRNA *	0.38 ± 0.19***	0.10 ± 0.03 ^{ns}	0.38 ± 0.15 ^{ns}	7.78 ± 0.88	0.10 ± 0.03	1.57 ± 0.41
Urine Ca/Crea (mol/mol)	13.12 ± 0.90 ^{ns}	11.88 ± 1.02 ^{ns}	0.45 ± 0.11 ^{ooo}	10.07 ± 2.60	8.71 ± 1.13	0.11 ± 0.11

Table S4. **Full set of biochemical data under high and low vitamin D and phosphate diets.** Low vitamin D content (“lowD”) = 0.3-0.5IU/g chow, high vitamin D content (“highD”) = 10IU/g chow, low phosphate content (“lowP”) = 0.1% P, high phosphate content (“highP”) = 1.2% P (for standard diet compare ¹¹ = 4.5IU/g chow vitamin D and 0.6% phosphate). “*” signs indicate significant differences between knockout and wild-type mice under lowP/highD diet. “oo” signs indicate statistically significant differences between knockout mice on lowP/lowD or highP/lowD diets, respectively, in comparison to knockout mice on lowP/highD. The levels of significance in the respective columns are indicated as follows: */^o = p<0.05, **/^{oo} = p<0.01, ***/^{ooo} = p<0.001, ns = non significant).

Supplemental references

1. Stark H, Eisenstein B, Tieder M, Rachmel A, Alpert G. Direct measurement of TP/GFR: a simple and reliable parameter of renal phosphate handling. *Nephron* 1986;44:125-8.
2. Brodehl J, Gellissen K, Weber HP. Postnatal development of tubular phosphate reabsorption. *Clin Nephrol* 1982;17:163-71.
3. Abecasis GR, Cherny SS, Cookson WO, Cardon LR. Merlin--rapid analysis of dense genetic maps using sparse gene flow trees. *Nat Genet* 2002;30:97-101.
4. Reshkin SJ, Forgo J, Murer H. Functional asymmetry of phosphate transport and its regulation in opossum kidney cells: phosphate transport. *Pflugers Arch* 1990;416:554-60.
5. Pfister MF, Lederer E, Forgo J, et al. Parathyroid hormone-dependent degradation of type II Na⁺/Pi cotransporters. *J Biol Chem* 1997;272:20125-30.
6. Ito N, Fukumoto S, Takeuchi Y, et al. Comparison of two assays for fibroblast growth factor (FGF)-23. *J Bone Miner Metab* 2005;23:435-40.
7. Fassbender WJ, Brandenburg V, Schmitz S, et al. Evaluation of human fibroblast growth factor 23 (FGF-23) C-terminal and intact enzyme-linked immunosorbent-assays in end-stage renal disease patients. *Clin Lab* 2009;55:144-52.
8. Smith ER, Ford ML, Tomlinson LA, et al. Instability of fibroblast growth factor-23 (FGF-23): implications for clinical studies. *Clin Chim Acta*. Netherlands: 2011 Elsevier B.V; 2011:1008-11.
9. Magen D, Berger L, Coady MJ, et al. A loss-of-function mutation in NaPi-IIa and renal Fanconi's syndrome. *N Engl J Med* 2010;362:1102-9.
10. Walton RJ, Bijvoet OL. Nomogram for derivation of renal threshold phosphate concentration. *Lancet* 1975;2:309-10.
11. Beck L, Karaplis AC, Amizuka N, Hewson AS, Ozawa H, Tenenhouse HS. Targeted inactivation of Npt2 in mice leads to severe renal phosphate wasting, hypercalciuria, and skeletal abnormalities. *Proc Natl Acad Sci U S A* 1998;95:5372-7.